ingegneria sismica
International Journal of Earthquake Engineering
Anno XLIII - Num. 2 - 2026

A Study on the Factors Affecting the Regulation Capability of Thermal Power Units Based on Factor Analysis

Ruichun Hou[1], *Hongfei Du*[1], *Jian Lv*[1], *Xiufeng Xing*[1] *and Xiaojun Li*[1,*]

1 Shanxi Century Pilot Electric Power Science and Technology Co., Ltd., Taiyuan, Shanxi, 030012, China

SUMMARY: *To further optimize and enhance the regulation capability of thermal power units, this study employs factor analysis to investigate relevant influencing factors. Building upon this foundation, it integrates LSTM networks and Bayesian optimization theory to propose a PA-mBO-LSTM prediction model for thermal power unit response to AGC regulation. This model is based on feature extraction and multi-level deep learning. The findings indicate that "rapid response capability," "control stability," "equipment health," and "cooperative optimization" are the four primary factors influencing thermal power unit regulation capability, with corresponding importance values of 0.343, 0.325, 0.248, and 0.196, respectively, exhibiting a decreasing order of influence. Validation using actual operational data from an 800MW unit demonstrates that the proposed model's prediction deviation remains within 15MW. Its prediction accuracy significantly outperforms models without feature extraction and single LSTM models, proving the model's capability to precisely evaluate thermal power units' response to AGC regulation under deep peak shaving conditions.*

KEYWORDS: *factor analysis; LSTM; Bayesian optimization; thermal power unit regulation capability; influencing factors*

1 Introduction

With the rigid growth in electricity demand, increasing challenges in optimizing the energy mix, evolving international dynamics, and the continuous advancement of the dual carbon strategy, the pace of clean and low-carbon transformation in the power system is accelerating. Wind and solar power, characterized by high uncertainty and low controllability, will gradually become the dominant sources of electricity. The share of thermal power generation capacity and output will continue to decline. However, the proportion of wind and solar power capacity remains lower than that of thermal power. Under the new power system operation, the flexible regulation capabilities of thermal power units must be further enhanced [1-5]. Thermal power units comprise key components such as boilers, steam turbines, and generators. The boiler converts fuel combustion into thermal energy, the steam turbine transforms thermal energy into mechanical energy, and the generator converts mechanical energy into electrical output. These components operate in coordination, and any malfunction in one link will affect the entire unit's operation [6, 7]. Thermal power units will play a crucial role in regulating and supporting future power systems, evolving further into flexible generation sources to effectively enhance system regulation capabilities. This regulation capacity directly impacts the grid's ability to integrate high proportions of renewable energy [8-10]. Demand for regulation capacity manifests

*Lxj_8104@163.com
https://doi.org/10.65102/is2026655
Published: 30 April, 2026

primarily in peak-shaving capacity and secondarily in ramping rates. Regarding peak-shaving capacity, given the limited scale of resources like pumped storage and adjustable loads, the depth of thermal power units' peak-shaving capability is critical. Online assessment of this deep peak-shaving capacity is essential to ensure renewable energy integration [11-13]. Simultaneously, the combined effect of renewable energy output and load variations—particularly during midday when photovoltaic generation peaks and electricity demand declines—demands that thermal units meet rapid load-response requirements. This is especially critical under new power supply security frameworks, where thermal units must swiftly adjust loads to meet grid regulation needs [14-17].

It is widely recognized that thermal power units should assume greater regulatory responsibilities. Research by Wang et al. [18] indicates that thermal power units with weak boiler heat storage capacity exhibit poor adaptability to deep frequency and peak load regulation, whereas circulating fluidized bed boilers and pulverized coal boilers with higher calorific values demonstrate the opposite characteristics. Shaoqiang et al. [19] revealed that factors such as combustion stability, operational reliability, environmental protection, and economic efficiency during low (variable) load operation of coal-fired boilers directly impact the deep peak shaving capability of coal-fired power generation units. Yin et al. [20] analyzed the impact of coal quality on coal-fired power generation units. Fluctuations in factors such as carbon, ash, and moisture content affect unit efficiency. In low-quality coal environments, unit efficiency declines, further impairing the unit's regulation capability.

Fuel quality affects combustion efficiency and rate. Lower calorific value fuels may slow heat generation in boilers, disrupting the entire regulation sequence and thereby impairing regulation capability [21, 22]. Xu et al. [23] concluded through simulation tests that both dynamic control characteristics and physical properties of thermal power plant boilers influence primary frequency regulation capability, though dynamic control characteristics exert a lesser impact. Zhang et al. [24] investigated the combustion characteristics of molten salt systems in coal-fired power plants, finding that compact molten salt systems enhance load change rates, thereby boosting peak-shaving benefits. Zhu et al. [25] demonstrated that optimal thermal load allocation methods influence thermal power plants' peak-shaving capabilities, with varying performance across different plant types. Han and He [26] applied a hybrid energy storage system combining battery storage and compressed air energy storage at specific power ratios to conventional coal-fired power plants, enhancing both peak shaving and frequency regulation capabilities. This improvement stems from the introduction of energy storage systems weakening the strong coupling between boilers and turbines in thermal power units, thereby affecting peak shaving and load variation capabilities [27]. Chen et al. [28] found that under deep peak shaving conditions, the primary frequency regulation characteristics of thermal power units were significantly improved, enhancing their frequency regulation capability.

Cong et al. [29] calculated Spearman's correlation coefficient and Pearson's correlation coefficient, indicating that factors such as reheater outlet pressure and flue gas temperature affect the peak shaving capability of thermal power units. In cold environments, equipment heat loss may increase, requiring more energy and time for unit regulation [30]. Ma et al. [31] proposed a comprehensive dynamic performance evaluation method to assess the peak-shaving characteristics of coal-fired power plants equipped with supercritical carbon dioxide (S-CO_2) cycles, revealing that S-CO_2 holds potential for enhancing peak load regulation. S-CO_2 generates electricity by pressurizing and heating carbon dioxide to its critical state [32]. This demonstrates that external environmental temperature and pressure resistance influence peak load regulation capability. Additionally, studies have evaluated thermal power units' regulation capabilities using metrics such as ramp rates and minimum load [33, 34]. Among these, only a

few explicitly identify influencing factors, lacking comprehensiveness. Furthermore, existing evaluations fail to quantify implicit factors like boiler characteristics and control systems, pay insufficient attention to correlations between indicators, and neglect coupling effects in multivariate environments. Factor analysis, a statistical method for identifying common factors among observed variables, effectively addresses these evaluation shortcomings. It simplifies data analysis by combining multiple observed variables into fewer independent variables (factors), uncovering underlying structures to explain relationships among observed variables [35, 36].

Based on factor analysis of factors influencing the regulation capability of thermal power units, this paper proposes the PA-mBO-LSTM prediction model, which integrates Bayesian optimization algorithms and LSTM networks. To validate the model's effectiveness, SPSS 28.0 optimal scale regression analysis was employed to measure the relationship between four independent variable factors—“rapid response capability,” “control stability,” “equipment health,” and “cooperative optimization”—and the dependent variable of thermal power unit AGC regulation capability. Finally, using a thermal power unit case study, the superiority of this model over other models is explored.

2 Study on Factors Affecting the AGC Regulation Capability of Thermal Power Units

Automatic Generation Control (AGC) plays a crucial role in coordinating the operation of boiler and turbine systems within thermal power units. It translates grid-issued regulation commands into various operational signals for the units, promptly adjusting generation deviations to minimize significant fluctuations in grid frequency. This system is vital for ensuring the safe and stable operation of the power grid. To enhance grid security and stability while improving the regulation efficiency of thermal power units, this paper first employs factor analysis (FA) to identify the key factors influencing the AGC regulation capability of thermal power units.

2.1 Factor Analysis Method

2.1.1 Basic Principles

The fundamental concept of factor analysis [37] is to group variables based on the magnitude of their correlations, placing highly correlated variables into the same group while ensuring lower correlations among variables within different groups. The underlying structure formed by each group of variables is termed a common factor. Its purpose is to reveal the intrinsic relationships among observed variables. While preserving as much original information as possible, it represents the original data structure with fewer dimensions, simplifying the data to uncover the essence of phenomena.

2.1.2 Mathematical Model

Suppose there are n samples $Z_1, Z_2, \ldots, Z_n$ and and P evaluation metrics $F_1, F_2, \ldots, F_p$, the mathematical model of factor analysis represents each sample as a linear weighted sum of $P < n$ common factors and one specific factor. That is:

$$\begin{cases} Z_1 = a_{11}F_1 + a_{12}F_2 + \cdots + a_{1p}F_p + \xi_1 \\ Z_2 = a_{21}F_1 + a_{22}F_2 + \cdots + a_{2p}F_p + \xi_2 \\ \cdots \\ Z_3 = a_{n1}F_1 + a_{n2}F_2 + \cdots + a_{np}F_p + \xi_n \end{cases} \tag{1}$$

Rewritten in matrix form:

$$\begin{pmatrix} Z_1 \\ Z_2 \\ \vdots \\ Z_n \end{pmatrix} = \begin{pmatrix} a_{11} & a_{12} & \cdots & a_{1n} \\ a_{21} & a_{22} & \cdots & a_{2n} \\ \cdots & \cdots & \cdots & \cdots \\ a_{n1} & a_{n2} & \cdots & a_{pn} \end{pmatrix} \cdot \begin{pmatrix} F_1 \\ F_2 \\ \vdots \\ F_p \end{pmatrix} + \begin{pmatrix} \xi_1 \\ \xi_2 \\ \vdots \\ \xi_n \end{pmatrix} \tag{2}$$

Abbreviated as:

$$Z = AF + \xi \tag{3}$$

Here, A is referred to as the factor loading matrix. Factor analysis replaces Z with F because $P < n$, thereby achieving the goal of reducing the dimensionality of variables.

The above factor model must satisfy the following fundamental assumptions:

(1) $P < n$.

(2) $COV(F, \xi) = 0$, i.e., F is uncorrelated with ε.

(3) $F = (F_1, F_2, \ldots, F_p)$ with $P < n$ and $F_1, F_2, \ldots, F_p$ are uncorrelated, with mean $E(F) = 0$, $COV(F) = \begin{pmatrix} 1 & & \\ & \ddots & \\ & & 1 \end{pmatrix} = I_\rho$ with covariance 1.

(4) $\xi = (\xi_1, \xi_2, ..., \xi_n)$ with $E(\xi) = 0$. The covariance matrix of ξ is diagonal, and $\xi_1, \xi_2, ..., \xi_n$ are mutually independent.

2.1.3 Solution Procedure

(1) Calculate the correlation matrix to determine whether the original variables are suitable for factor analysis. Factor analysis requires strong correlations among the original variables; if the variables are mutually independent, factor analysis is unnecessary. SPSS software provides several tests to assess whether variables are appropriate for factor analysis.

1) Mirrored Correlation Matrix Test

Partial correlation coefficients serve as an alternative measure of variable interdependence. Key characteristics include: First, when variables share common factors, partial correlation coefficients between variable pairs should decrease after controlling for linear effects of other variables. Second, when factor analysis assumptions hold, partial correlation coefficients serve as estimates of correlations between latent factors and should approach zero, as latent factors are assumed to be mutually independent. This can be assessed by examining the proportion of inverse correlation coefficients (i.e., the complement of partial correlation coefficients) within the matrix; an excessively large proportion indicates unsuitability.

2) Bartlett's Sphericity Test

This test determines whether the data originate from a multivariate normal distribution population. Its null hypothesis is that “the correlation matrix is a unit matrix.” If the F-value is

significant in the difference test, it indicates the matrix is not a unit matrix and the data originate from a multivariate normal distribution population, allowing further analysis. Otherwise, analysis is not feasible.

3) KMO Test

This test compares the relative magnitudes of simple correlation coefficients and partial correlation coefficients among observed variables, yielding values ranging from 0 to 1. When the sum of squares of partial correlation coefficients among all variables is significantly smaller than the sum of squares of simple correlation coefficients, the KMO value approaches 1. A KMO value above 0.8 indicates suitability for factor analysis, while a lower value suggests unsuitability. KMO value interpretations: 0.90, 0.80, 0.70, 0.60, 0.50, <0.50 correspond to excellent, suitable, fair, less suitable, poor, unacceptable, respectively.

(2) Factor Extraction: Calculate the factor loading matrix using a specific method. Factor loadings refer to the weighted coefficients a_{ij} of each common factor in the factor analysis model for the observed variables. Typically, the coefficients of common factors are termed factor loadings, i.e., the coefficients within the factor analysis model. Representing all factor loadings in matrix form yields the factor loading matrix.

(3) Determine the number of common factors required to describe the data based on specific rules. Common rules for determining the number of common factors include:

1) Based on the cumulative percentage of total variance explained by common factors, typically exceeding 85%.

2) Factors with eigenvalues greater than 1 can be selected for inclusion in the number of common factors. Eigenvalues represent the degree of variation in factors; during factor extraction, common factors with the largest eigenvalues are usually extracted first.

3) After sorting eigenvalues in descending order, factors whose cumulative product exactly exceeds 1 may be included in the common factor count.

4) When the number of variables P is even, the number of common factors should be less than $P/2$. When P is odd, it should be less than $(P-1)/2$.

5) Based on the scree plot, rank factors by their eigenvalues. Typically, the scree plot exhibits a distinct inflection point. Factors before this point are major factors, while those after are minor factors.

(4) Factor Interpretation and Factor Rotation

Factor interpretation typically involves ranking variables with different loadings on the same factor. Variables with small factor loadings are removed from that factor, generally using a threshold of loadings less than 0.5.

The factor loading matrix is not unique. Multiply the initial factor loading matrix A by an orthogonal matrix T on the right:

$$(AT)(AT)' = A(TT')A' = AA' = R \tag{4}$$

We refer to this transformation method A as factor rotation, whose purpose is to maximize the polarization of each observation vector's projection onto the new coordinate axes toward the 1 and 0 extremes. Factor rotation methods include orthogonal rotation, oblique rotation, and others.

2.2 Analysis of Influencing Factors Based on Factor Analysis

2.2.1 Influencing Factor Indicators and Data Sources

Drawing on the indicators selected by relevant scholars to study the AGC response ability of thermal power units, and according to the characteristics of the index data, the representativeness and scientific principles of the research objects, and the characteristics of thermal power units, the maximum load lift rate of the unit (X_1), the maximum load reduction rate of the unit (X_2), the average tracking error of AGC instructions (X_3), the contribution of primary frequency regulation (X_4), the heat storage capacity index (X_5), the standard deviation of the main steam pressure fluctuation (X_6), the sensitivity of feed water flow regulation (X_7), Fifteen initial indicators, including the coal calorific value uniformity coefficient (X_8), the delay time constant of the coal mill (X_9), the DCS closed-loop control period (X_{10}), the nonlinearity of the steam turbine gate stem stroke (X_{11}), the operation rate of the coordinated control system (X_{12}), the number of historical AGC rejections (X_{13}), the uniformity of the ammonia spraying grid of the denitrification device (X_{14}), and the vacuum tightness of the condenser (X_{15}) were taken as the research objects, and the data corresponding to these indicators were normalized to make each index within the same scale range to allow for subsequent factor analysis. The indicator data comes from the actual operation records of multiple thermal power plants in a certain region, covering the detailed operating parameters of thermal power units of different models and capacities over a period of time.

2.2.2 Applicability Test

To eliminate inconsistencies in the raw data, it underwent standardization. The suitability of the standardized indicator data was assessed through KMO and Bartlett's tests, with results shown in Table 1. The KMO value was 0.724 > 0.5, and Sig. = 0.000 < 0.05, indicating that the data is suitable for factor analysis.

Table 1: KMO and Bartlett test values

A measure of adequacy of the Kaiser-Meyer-Olkin sample		0.724
Bartlett's sphericity test	Approximate chi-square	427.431
	df	78.000
	Sig.	0.000

2.2.3 Factor Analysis Process and Results

Factor analysis was performed on the standardized data, yielding the total variance explained as shown in Table 2. Based on the principle of eigenvalues greater than 1, four common factors—F_1, F_2, F_3, and F_4—were extracted. At this point, the variance explained by these four common factors reached 86.50%, exceeding the threshold of 85%. This indicates that selecting these four common factors can fundamentally represent the AGC regulation capabilities of thermal power units across multiple thermal power plants in the region.

Table 2: Explanation of total variance

Module	Initial eigenvalue			Extract the sum of squared loads			Rotating load sum of squares		
	Total	Percentage of variance /%	Cumulative /%	Total	Percentage of variance /%	Cumulative /%	Total	Percentage of variance /%	Cumulative /%
1	5.794	38.63	38.63	5.794	38.63	38.63	5.624	37.49	37.49
2	3.525	23.50	62.13	3.525	23.50	62.13	3.232	21.55	59.04
3	2.253	15.02	77.15	2.253	15.02	77.15	2.458	16.39	75.43
4	1.402	9.35	86.50	1.402	9.35	86.50	1.661	11.07	86.50
5	0.518	3.45	89.95						
6	0.424	2.83	92.78						
7	0.345	2.30	95.08						
8	0.283	1.89	96.97						
9	0.212	1.41	98.38						
10	0.126	0.84	99.22						
11	0.059	0.39	99.61						
12	0.034	0.23	99.84						
13	0.014	0.09	99.93						
14	0.009	0.06	99.99						
15	0.002	0.01	100						

To obtain clearer results from the factor analysis, orthogonal factor rotation was further applied to more explicitly refine the factor structure. Factor rotation involves rotating the initial factor loading matrix to redistribute the relationships between factors and original variables, making the coefficients in the factor loading matrix more significant. Simply put, this process amplifies large factors and reduces small ones, thereby facilitating easier factor interpretation and aiding in the selection of variables that best represent the factors. The rotated factor component matrix is presented in Table 3.

By examining the factor loadings, it is evident that the first common factor F_1 exhibits loadings exceeding 0.75 on X_1, X_2, X_3, X_4, and X_5. This indicates that factor F_1 strongly explains the variability in indicators X_1, X_2, X_3, X_4, and X_5, all of which are related to the speed and accuracy of thermal power units responding to AGC. Therefore, this factor can be named the "Rapid Response Capability" factor. The second principal factor F_2 exhibits loadings of 0.95, 0.88, 0.77, 0.76, and 0.64 on indicators X_6, X_7, X_{10}, X_{11}, and X_{12}, respectively. These five indicators reflect the closed-loop control system's disturbance rejection capability and robustness, justifying its designation as the "Control Stability" factor. The third factor F_3 has loadings of 0.88, 0.85, 0.60, 0.76, and 0.66 on indicators X_8, X_9, X_{13}, X_{14}, and X_{15} respectively. Specifically, these indicators relate to potential equipment failure risks, thus this factor can be named the "Equipment Health" factor. The fourth principal component F_4 exhibits loadings exceeding 0.7 for both X_{14} and X_{15}, with relatively high loadings of 0.36 and 0.28 respectively on these indicators. These metrics reflect the collaborative efficiency between environmental protection equipment and the main system, thus it is named the "Collaborative Optimization Factor."

Table 3: Factor component matrix after rotation

Variables	Component			
	F_1	F_2	F_3	F_4
X_1	**0.94**	0.14	-0.07	0.02
X_2	**0.92**	0.15	-0.13	0.05
X_3	**0.87**	-0.07	0.05	-0.13
X_4	**0.90**	-0.25	0.09	-0.03
X_5	**0.78**	-0.33	0.27	0.12
X_6	0.10	**0.95**	-0.07	0.08
X_7	0.09	**0.88**	0.19	-0.15
X_8	-0.08	0.09	**0.88**	0.08
X_9	-0.13	0.09	**0.85**	0.19
X_{10}	0.05	**0.77**	-0.22	0.36
X_{11}	-0.23	**0.76**	0.32	-0.20
X_{12}	0.18	**0.64**	0.43	0.28
X_{13}	-0.35	0.54	**0.60**	-0.29
X_{14}	0.28	0.16	**0.76**	**0.81**
X_{15}	0.38	0.21	**0.66**	**0.73**

2.2.4 Analysis of Impact Factor Influence Levels

Data analysis ultimately employed SPSS 28.0 optimal scaling regression analysis to measure the relationship between the four independent variable factors identified earlier and the AGC regulation capability of thermal power units. Optimal scaling is a method capable of extending the applicability of various traditional analytical approaches to all measurement scales, enabling simultaneous regression analysis, factor analysis, and other techniques for unordered categorical variables, ordered categorical variables, and continuous variables. Applying the optimal scale method to linear regression yields optimal scale regression analysis.

The ANOVA results obtained from SPSS are presented in Table 4. Similar to conventional regression analysis, Table 4 shows the significance test for the overall model. It indicates that the data transformed through optimal scaling possesses statistical significance.

Table 4: Anova analysis

Calculation result	Sum of squares	df	Equal square	F	Sig.
Regression	34.329	4	11.826	14.418	0.000
Residuals	126.514	148	0.915	-	-
Total	160.843	152	12.741	-	-

The estimated values and test results for each coefficient in the regression model are shown in Table 5. It can be seen that the relationship between the quantitative scores of the four independent variables and the quantitative scores of the dependent variable is statistically significant.

Table 5: Coefficient tests in the model

AGC regulation capacity factor	Standard coefficient		df	F	Sig.
	Beta	Bootstrap (1000) estimation of standard error			
Rapid response capability factor	0.272	0.072	1	15.274	0.000
Control stability factor	0.231	0.078	1	7.635	0.004
Equipment health factor	0.245	0.086	1	9.453	0.007
Collaborative optimization factor	0.287	0.088	1	13.126	0.002

The specific results of the optimal scale regression analysis are shown in Table 6. The importance index indicates that the higher the value, the more significant the variable is in predicting the dependent variable, with the sum of all item values equaling 1. It can be observed that the rapid response capability factor exerts the greatest influence on the dependent variable, followed by the control stability factor, equipment health factor, and collaborative optimization factor, with corresponding importance values of 0.343, 0.325, 0.248, and 0.196, respectively. These four factors exert varying degrees of influence on the dependent variable. Additionally, tolerance indicates the ability of a variable to influence the dependent variable in ways that cannot be explained or replaced by other independent variables. Higher values are preferable. In this study, the tolerance values for all four independent variable factors exceed 0.99, indicating that the four factors are nearly uncorrelated and influence the dependent variable from distinct perspectives. The results of the optimal scale regression analysis are thus considered reliable.

Table 6: Optimal scale regression analysis results

AGC regulation capacity factor	Zero order	Partial	Part	Importance	Tolerance	
					Before conversion	After conversion
Rapid response capability factor	0.281	0.294	0.274	0.343	0.997	0.997
Control stability factor	0.242	0.251	0.228	0.325	0.995	0.995
Equipment health factor	0.273	0.267	0.246	0.248	0.994	0.994
Collaborative optimization factor	0.298	0.325	0.302	0.196	0.996	0.996

3 Evaluation of Thermal Power Unit Regulation Capability Based on PA-BO-LSTM

Based on the influencing factors of thermal power units' AGC regulation capability, this chapter employs Bayesian optimization (BO) theory to construct an evaluation model for thermal power units' AGC regulation capability based on PA-BO-mLSTM. This model provides data support for enhancing the AGC regulation capability of thermal power units.

3.1 LSTM Neural Networks

Long Short-Term Memory (LSTM) [38] is a variant of Recurrent Neural Networks (RNN). It is a temporal recurrent neural network architecture designed to address issues such as gradient

vanishing and gradient explosion that commonly arise when RNNs process long sequence data. The LSTM neural network primarily consists of one input layer, one output layer, and several hidden layers. The hidden layers incorporate three types of gate structures and a memory cell, which is responsible for storing state information and propagating it forward. The three gates are the forget gate, the input gate, and the output gate. The unit structure is illustrated in Figure 1.

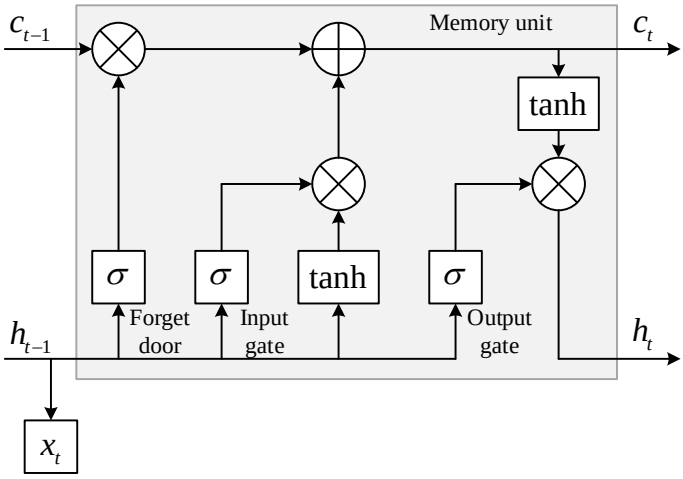

Figure 1: Structure diagram of the LSTM unit

3.2 Bayesian Optimization Theory

The number of hidden layer neurons and the learning rate in LSTM network models significantly impact the training efficiency and performance of neural networks. An appropriate L2 regularization strength can prevent model overfitting. Selecting a suitable combination of hidden layer neuron count, learning rate, and L2 regularization strength is crucial for LSTM network models. Bayesian optimization [39] minimizes the objective function by leveraging prior evaluations based on the objective function itself, particularly when only a finite number of sample points are available. This approach effectively addresses the challenge of determining the corresponding functional relationship for LSTM network model parameters.

3.3 Development of a Prediction Model for AGC Regulation Capability of Thermal Power Units

3.3.1 Model Parameter Selection Based on Factor Analysis

Through mechanism analysis, the power deficit ΔP of thermal power units was selected as the model's output variable to characterize AGC regulation capability. Factor analysis was employed to screen characteristic variables, with corresponding thermal power unit parameters selected as input variables.

3.3.2 BO-LSTM Prediction Model Framework

The LSTM network model constructed in this paper is a single-hidden-layer network model. To enhance the model's prediction accuracy, the parameters of the LSTM network are optimized using the BO algorithm, thereby establishing the BO-LSTM network prediction model. Its structure is shown in Figure 2. The process of utilizing BO to optimize the LSTM is illustrated in Figure 3. The specific steps are as follows:

(1) Initialize the LSTM network's hyperparameters, specifically including the number of neurons in the hidden layer, learning rate, and L2 regularization strength. Their respective value ranges are [50, 200], [10^{-5}, 10^{-1}], and [10^{-10}, 10^{-2}]. Randomly select sampling points within these ranges to construct a set of sampling points.

(2) $D=\{(x_1,y_1),(x_2,y_2),\cdots,(x_n,y_n)\}$

(3) Update the Gaussian process model and obtain the posterior distribution of the function based on the Gaussian process model $f(x)$. Select the next sampling point x_{n+1} by maximizing the value of the acquisition function, and compute the objective function value y_{n+1} at the evaluation point x_{n+1}.

(4) Add the new sample (x_n+1, y_n+1) to the historical sample set D and update the Gaussian model to better approximate the true distribution of the objective function.

(5) When the iteration count is reached, the model stops updating and outputs the optimal parameter set. Otherwise, return to step (2) to continue iteration, where the iteration count is set to 50.

(6) Input the obtained optimal parameter set into the LSTM network for training to obtain the BO-LSTM network model.

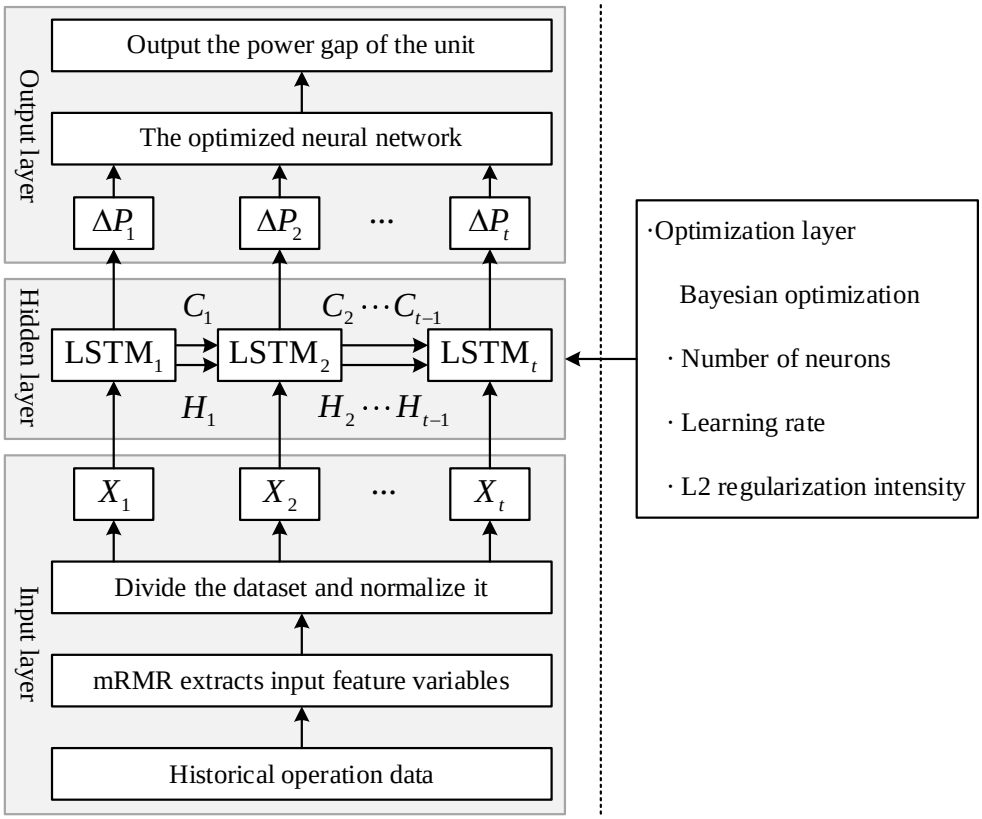

Figure 2: BO-LSTM network model

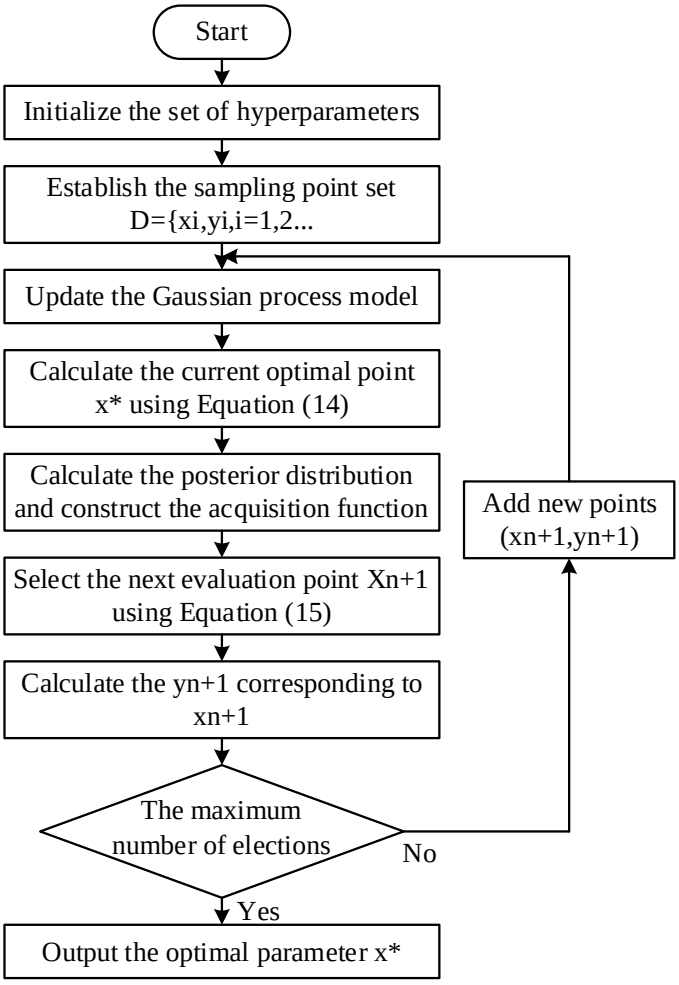

Figure 3: Flowchart of BO optimization

3.3.3 PA-BO-LSTM Power Shortfall Prediction Model

After feature extraction via factor analysis, the following variables are used as inputs: actual power output P of the thermal power unit, AGC command P_n, main steam pressure p_0, feedwater flow rate q, total valve opening angle r, and governor stage pressure p_g. The response process of a thermal power unit to an AGC command depends on historical values. Taking the prediction at time t as an example, first, use the following historical values as model inputs: $[t-k, t-1]$ main steam pressure, p_0 feedwater flow rate, q total valve opening, r governor stage pressure, p_g actual unit power output P from the previous time step, and P_n the current AGC command. This predicts the values of these parameters at the current time t. Then, use these predicted values as new model inputs to obtain the unit's actual power output and deficit at the current time. Following this process, by inputting the predicted time sequence and corresponding AGC commands, we can forecast the power deficit of thermal units over the $[t+1, t+T]$-time period. This represents the thermal units' response capability to a given AGC command—that is, their regulation capacity.

3.4 Case Study Analysis

Taking an 800MW supercritical coal-fired unit as an example, AGC regulation experiments were conducted under deep peak-shaving conditions. Relevant unit operation data were

collected at 1-second intervals, with abnormal data such as operational faults excluded. The resulting AGC regulation data are shown in Figure 4. Figure 4 shows a total of 2,340 samples encompassing three load ramping processes. Specifically: Samples 1–284 represent a 20MW upward ramp, Samples 490–623 represent a 20MW downward ramp, Samples 1533–1861 represent a 40MW upward ramp, samples 870–1100 represent a 40MW load increase process, samples 1210–1415 represent a 40MW load decrease process, samples 1533–1861 represent a 60MW load increase process, and samples 1977–2340 represent a 60MW load decrease process. The time scale for power prediction was set to the duration of a single load increase/decrease event.

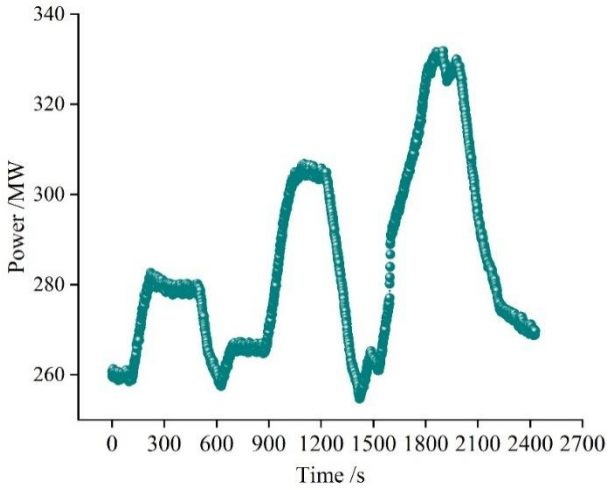

Figure 4: AGC regulates data

The data was processed using the Z-score standardization method to conform to a standard normal distribution, with a mean of 0 and a standard deviation of 1. The data processing function is:

$$x' = \frac{x - \mu}{\sigma} \tag{5}$$

In the formula: x' denotes the normalized data, μ represents the sample mean, and σ denotes the sample standard deviation.

The AGC adjustment process data for 20MW increases/decreases, 40MW increases/ decreases, and 60MW increases were used as the training set to train the BO-LSTM neural network. The 60MW decrease data served as the test set to evaluate the predictive accuracy of the AGC capability identification model. The first layer of the BO-LSTM network predicts main steam pressure, valve opening, and main steam flow rate, while the second layer predicts the final actual power output. To validate the accuracy of the proposed method, both a single BO-LSTM network and an mBO-LSTM network were employed to predict the AGC power regulation capability of thermal power units. The power prediction results and errors for each model are shown in Figures 5 and 6, respectively. It can be observed that: the prediction curve of the PA-mBO-LSTM model nearly overlaps with the actual value curve. The use of factor analysis to screen model variables ensures more scientific parameter selection. The mBO-LSTM network model maximizes the simulation of coordinated unit control conditions. Each memory unit in the BO-LSTM evaluates and filters data, thereby ensuring prediction stability. The absolute error between the turbine's actual output power and the model's predicted values remains within 15 MW, demonstrating the model's high accuracy in power prediction. The

power prediction results from the single BO-LSTM neural network deviate significantly from the actual power, primarily because a single model cannot adequately fit the coordinated control conditions of the units, resulting in a prediction error of 20 MW. The mBO-LSTM neural network achieves higher precision than the standalone BO-LSTM network. However, without factor analysis of input and output variables, its prediction accuracy remains insufficient, with errors still exceeding those of the PA-mBO-LSTM network model.

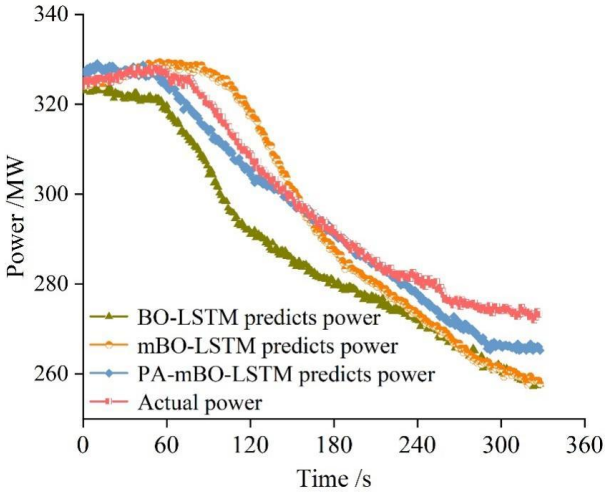

Figure 5: Power prediction results of each model

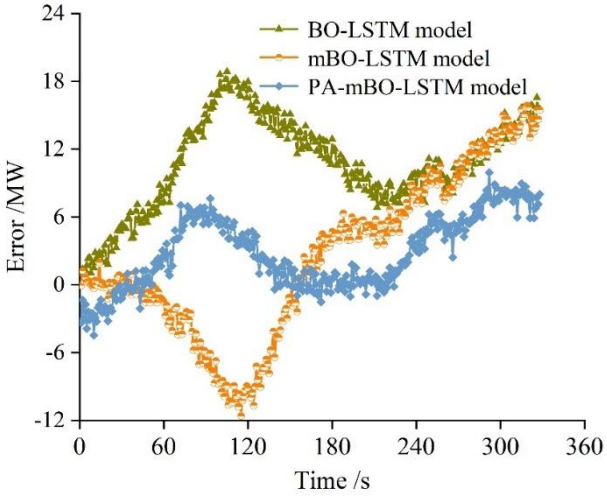

Figure 6: Power prediction errors of each model

The model's identification performance is evaluated using the mean relative error, root mean square error, and normalized root mean square error as metrics. The definitions of each metric are as follows:

$$ARE = \frac{1}{n}\sum_{i=1}^{n}\frac{|\hat{W}_i - W_i|}{W_{\max} - W_{\min}} \times 100\% \tag{6}$$

$$RMSE = \sqrt{\frac{1}{n}\sum_{i=1}^{n}(\hat{W}_i - W_i)^2} \tag{7}$$

$$NRMSE = \frac{1}{\bar{w}}\sqrt{\frac{1}{n}\sum_{i=1}^{n}(\hat{W}_i - W_i)^2} \times 100\% \tag{8}$$

In the equation: $\bar{W}$ denotes the average value of actual power output, $W_{\max}, W_{\min}$ represent the maximum and minimum values of actual power output, respectively, and n is the number of samples in the test set.

The prediction errors of different models are shown in Table 7. The PA-mBO-LSTM model achieved ARE, RMSE, and NRMSE values of 2.1%, 0.21 MW, and 2.4% on the training set, and 2.9%, 0.32 MW, and 3.4% on the test set. To validate model accuracy, an LSTM neural network model was established using thermal power unit operational data for comparison. Results indicate that the error of the PA-mBO-LSTM network model is significantly lower than that of the LSTM, mLSTM, BO-LSTM, and mBO-LSTM network models, demonstrating that the PA-mBO-LSTM model possesses high prediction accuracy and excellent forecasting performance.

Table 7: Prediction error of the models

Model	Training set			Test set		
	ARE /%	RMSE /%	NRMSE /%	ARE /%	RMSE /%	NRMSE /%
LSTM	3.7	0.43	3.9	4.0	0.52	4.8
mLSTM	3.4	0.36	3.6	3.5	0.43	4.0
BO-LSTM	3.5	0.38	3.7	3.8	0.47	4.5
mBO-LSTM	2.5	0.24	3.2	3.1	0.38	3.7
PA-mBO-LSTM	2.1	0.21	2.4	2.9	0.32	3.4

The power command and power forecast data are shown in Figure 7. Based on the data in Figure 7, the AGC response time for this thermal power unit is calculated to be 22 seconds, with a regulation rate of 1.79 MW/s and a regulation accuracy of 7.2473 MW.

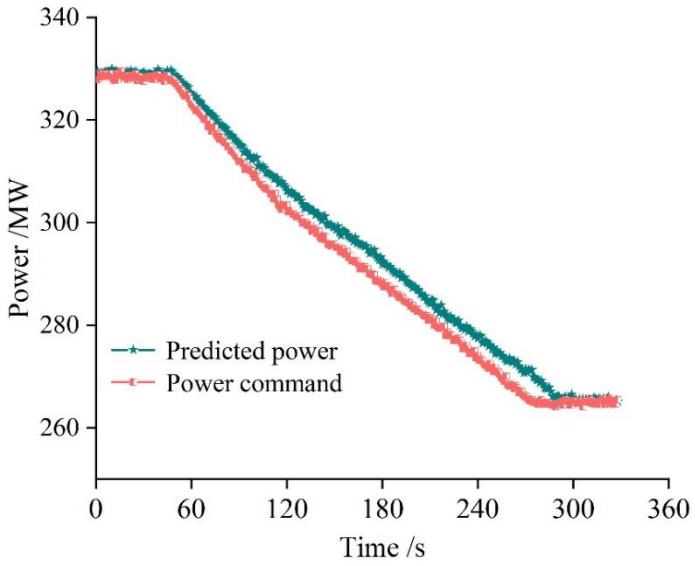

Figure 7: Power command and power prediction value

4 Conclusion

This paper investigates the influencing factors of thermal power unit regulation capability using factor analysis and proposes the PA-mBO-LSTM prediction model for thermal power unit regulation capability.

Through factor analysis, four common factors—F_1, F_2, F_3, and F_4—were extracted, explaining 86.50% cumulative variance (exceeding 85%), which fundamentally represents the AGC regulation capability of thermal power units across multiple thermal power plants in the region. The four common factors were named “Rapid Response Capability,” “Control Stability,” “Equipment Health,” and “Cooperative Optimization” based on their loadings for corresponding influencing factors, with respective importance values of 0.343, 0.325, 0.248, and 0.196.

When validated on an actual 800MW unit case, the proposed model demonstrated a prediction deviation within 15MW, outperforming the 20MW deviation of the standalone BO-LSTM model. The PA-mBO-LSTM model achieved ARE, RMSE, and NRMSE values of 2.1%, 0.21 MW, and 2.4% on the training set, and 2.9%, 0.32 MW, and 3.4% on the test set, demonstrating significantly higher accuracy than other comparison models. Based on the model's prediction accuracy data, the AGC response time for the case study thermal power unit was calculated as 22 seconds, with a regulation rate of 1.79 MW/s and a regulation accuracy of 7.2473 MW.

About the Author

Ruichun Hou (1972.2), male, born in Taiyuan, Shanxi, assistant chief engineer, works at Shanxi Century Pilot Electric Power Science and Technology Co., Ltd. In recent years, Hou has mainly engaged in research on energy-saving technologies and technological innovation of thermal power generating units.

Hongfei Du (1990.11), male, born in Wutai, Shanxi, director of the Thermal Power Technology Service Center, works at Shanxi Century Pilot Electric Power Science and Technology Co., Ltd. In recent years, Du is mainly engaged in research on process control of thermal power generating units.

Jian Lv (1992.06), male, born in Wenshui, Shanxi, thermal control engineer, works at Shanxi Century Pilot Electric Power Science and Technology Co., Ltd. In recent years, Lv is mainly engaged in the research of control optimization of thermal power generating units.

Xiufeng Xing (1981.4), male, born in Wutai, Shanxi, deputy general manager, works at Shanxi Century Pilot Electric Power Science and Technology Co., Ltd. In recent years, Xing has mainly engaged in boiler technology and application in thermal power generating units.

Xiaojun Li (1981.4), male, born in Shanyin, Shanxi, director of the Power Center, works at Shanxi Century Pilot Electric Power Science and Technology Co., Ltd. In recent years, Li is mainly engaged in chemical technology and protection application for thermal power generating units.

Ronggui Zhang (1989.6), male, born in Qingdao, Shandong, project manager, works at Shandong Luruan Digital Technology Co., Ltd. In recent years, Zhang has mainly engaged in coordinated interaction control of generation units, load, and storage.

References

[1] Wang, J., Song, C., & Yuan, R. (2021). CO2 emissions from electricity generation in

China during 1997–2040: the roles of energy transition and thermal power generation efficiency. Science of The Total Environment, 773, 145026.

[2] Tong, J., Liu, W., Mao, J., & Ying, M. (2022). Role and development of thermal power units in new power systems. IEEE Journal of Radio Frequency Identification, 6, 837-841.

[3] Xu, Y., Liu, W., & Yang, B. (2024). Coordinated planning of thermal power, wind power, and photovoltaic generator units considering capacity electricity price. IET Renewable Power Generation, 18(14), 2539-2559.

[4] Chen, S., Liu, P., & Li, Z. (2020). Low carbon transition pathway of power sector with high penetration of renewable energy. Renewable and Sustainable Energy Reviews, 130, 109985.

[5] Jiang, N., Zhang, C., Su, W., Jin, H., & Balezentis, T. (2024). Towards carbon-neutral society: Reconciling peak carbon strategy and thermal power generation via regional eco-efficiency analysis. Sustainable Development, 32(4), 2944-2961.

[6] Panchal, D., & Kumar, D. (2017). Maintenance decision-making for power generating unit in thermal power plant using combined fuzzy AHP-TOPSIS approach. International Journal of Operational Research, 29(2), 248-272.

[7] Andervazh, M. R., & Javadi, S. (2017). Emission-economic dispatch of thermal power generation units in the presence of hybrid electric vehicles and correlated wind power plants. IET Generation, Transmission & Distribution, 11(9), 2232-2243.

[8] Li, C., Feng, C., Li, J., Hu, D., & Zhu, X. (2023). Comprehensive frequency regulation control strategy of thermal power generating unit and ESS considering flexible load simultaneously participating in AGC. Journal of Energy Storage, 58, 106394.

[9] Kang, J., Chen, X., Yang, Z., Liu, L., You, M., Zhao, Y., ... & Hong, F. (2024). Performance enhancement and optimization of primary frequency regulation of coal-fired units under boundary conditions. Energy Science & Engineering, 12(5), 2209-2219.

[10] Lv, Z., Liu, X., Liu, Z., Jiang, Z., Lin, Z., Zhao, Z., & Han, X. (2023). Dynamic simulation study of the secondary frequency regulation of a 1000 MW thermal power unit assisted by flywheel energy storage. AIP Advances, 13(4).

[11] WANG, H. X., ZHOU, Z. C., GUI, B., LV, Q., & LI, W. D. (2017). Compensation model of deep peak load regulation of thermal power units with flexibility reform. power, 1, 3.

[12] Wang, J., Huo, J., Zhang, S., Teng, Y., Li, L., & Han, T. (2021). Flexibility transformation decision-making evaluation of coal-fired thermal power units deep peak shaving in China. Sustainability, 13(4), 1882.

[13] Wei, W. A. N. G., Jing, X. U., Xiang, Z. H. A. O., Xiaojiang, Y. U. A. N., & Zhenxin, L. I. (2025). < trans-title> Analysis on Peak Load Regulation Status Quo for Coal-fired Power Plants in China. Southern Energy Construction, 4(1), 18-24.

[14] Zhou, J., Zhang, L., Zhu, L., & Zhang, W. (2024). A data-driven operating improvement method for the thermal power unit with frequent load changes. Applied Energy, 354,

122195.

[15] Zeng, R., Zhang, X., Deng, Y., Li, H., & Zhang, G. (2020). Optimization and performance comparison of combined cooling, heating and power/ground source heat pump/photovoltaic/solar thermal system under different load ratio for two operation strategies. Energy Conversion and Management, 208, 112579.

[16] Li, J., Liao, D., Li, H., Li, W., & Zhang, Y. (2019, July). Research and implementation of rapid load regulation of thermal power units based on large-scale renewable energy. In IOP Conference Series: Earth and Environmental Science (Vol. 295, No. 5, p. 052037). IOP Publishing.

[17] Li, G., Du, G., Liu, G., & Yan, J. (2024). Study on the dynamic characteristics, control strategies and load variation rates of the concentrated solar power plant. Applied Energy, 357, 122538.

[18] Wang, J., Zhong, J., & Gou, X. (2018). Control strategy study on frequency and peak-load regulation of coal-fired power plant based on boiler heat storage capacity. Proceedings of the Institution of Mechanical Engineers, Part A: Journal of Power and Energy, 232(8), 1063-1078.

[19] Shaoqiang, Z. H. A. N. G., Lu, C. H. E. N., Ziyi, L. I. U., Peng, Z. H. A. N. G., Zhibo, W. A. N. G., & Minhang, S. O. N. G. (2022). Discussion on key problems of depth peak adjustment for large coal-fired boilers. Southern Energy Construction, 9(3), 16-28.

[20] Yin, J., Liu, M., Zhao, Y., Wang, C., & Yan, J. (2021). Dynamic performance and control strategy modification for coal-fired power unit under coal quality variation. Energy, 223, 120077.

[21] Yang, C., Hao, X., Zhang, Q., Chen, H., Yin, Z., & Jin, F. (2023). Performance analysis of a 300 MW coal-fired power unit during the transient processes for peak shaving. Energies, 16(9), 3727.

[22] Yin, J., Liu, M., & Yan, J. (2022). Effect of fuel side deviations on the load-cycling performance of thermal power plants: A dynamic simulation. Applied Thermal Engineering, 206, 118041.

[23] Xu, D., Hao, L., Chen, L., Qi, X., Liu, Y., Li, J., ... & Xu, F. (2024, September). Influence of Boiler Model on Simulation of Primary Frequency Regulation of Thermal Power Units. In 2024 The 9th International Conference on Power and Renewable Energy (ICPRE) (pp. 985-989). IEEE.

[24] Zhang, X., Ma, Z., Wen, H., Yang, Z., & Liu, H. (2024). Study on the characteristics of molten salt heat storage in the fast peak regulation of coal-fired power unit. Thermal Science, 28(5 Part A), 3825-3834.

[25] Zhu, L., Wang, Q., Zheng, W., Guo, Y., Han, Y., Guo, J., ... & Shang, P. (2019, December). Research on Heat Load Distribution Based on Peaking Capacity of Thermal Power Plant. In IOP Conference Series: Materials Science and Engineering (Vol. 677, No. 4, p. 042085). IOP Publishing.

[26] Han, X., & He, P. (2025). Research on the configuration and operation of peak and frequency regulation of hybrid energy storage system assisting a coal-fired power plant. Journal of Energy Storage, 127, 117134.

[27] Zhang, K., Liu, M., Zhao, Y., Yan, H., & Yan, J. (2022). Design and performance evaluation of a new thermal energy storage system integrated within a coal-fired power plant. Journal of Energy Storage, 50, 104335.

[28] Chen, Z., Qin, T., Zhang, Z., & Liu, L. (2021, November). Study of primary frequency regulation characteristics for thermal power units under deep peak shaving condition. In 2021 2nd International Conference on Artificial Intelligence and Computer Engineering (ICAICE) (pp. 850-854). IEEE.

[29] Cong, R., Wei, L., Fu, Y., & Li, J. (2024, May). Research on the Sensitivity Analysis of Peaking Capacity of Coal-fired Units and Operation Adjustment Decision-making in the Novel Power System. In 2024 3rd International Conference on Energy, Power and Electrical Technology (ICEPET) (pp. 637-640). IEEE.

[30] Feng, H., Wang, M., Wang, N., Xu, Y., He, S., & Gao, M. (2022). Influence of environmental parameters on the cold-end and thermal system of coal-fired power plant based on Ebsilon simulation. Thermal Science and Engineering Progress, 32, 101340.

[31] Ma, T., Li, M. J., Xue, X. D., Guo, J. Q., Wang, W. Q., & Jiang, T. (2023). Study of Peak-load regulation characteristics of a 1000MWe S-CO2 Coal-fired power plant and a comprehensive evaluation method for dynamic performance. Applied Thermal Engineering, 221, 119892.

[32] Xu, J., Liu, C., Sun, E., Xie, J., Li, M., Yang, Y., & Liu, J. (2019). Perspective of S− CO2 power cycles. Energy, 186, 115831.

[33] Al-Bahrani, L., Seyedmahmoudian, M., Horan, B., & Stojcevski, A. (2021). Solving the real power limitations in the dynamic economic dispatch of large-scale thermal power units under the effects of valve-point loading and ramp-rate limitations. Sustainability, 13(3), 1274.

[34] Umrao, O. P., Kumar, A., & Saini, V. K. (2017). Performance of coal based thermal power plant at full load and part loads. Glob. J. Technol. Optim, 8(01), 1-5.

[35] Shrestha, N. (2021). Factor analysis as a tool for survey analysis. American journal of Applied Mathematics and statistics, 9(1), 4-11.

[36] Zheng, X., Yang, X., Miao, H., Liu, H., Yu, Y., Wang, Y., ... & You, S. (2022). A factor analysis and self-organizing map based evaluation approach for the renewable energy heating potentials at county level: A case study in China. Renewable and Sustainable Energy Reviews, 165, 112597.

[37] Hui Wang, Su Zhang, Hanya Dai, Mingxin Gong, Ningxiang Zou, Feng Jia & Lejun Wang. (2025). Investigating the key influencing factors of pre-jump height in juvenile trampoline gymnasts using grey relational analysis. Frontiers in Psychology,16,1596942-1596942.

[38] Hongling Ding, Lihong Li, Gaojie Jia, Chunlei Zhao, Jianxin Li,Shuai Yan... & Fusheng Wang. (2025). Research on coal spontaneous combustion temperature prediction model based on BO-LSTM. Process Safety and Environmental Protection,201(PB),107570-107570.

[39] Ren jie Wu, Yu zhou Wang, Khant Swe Hein & Jin Xia. (2025). An enhancement method for chloride diffusion coefficient long-term prediction based on Hilbert dynamic probabilistic interpolation and BO-LSTM. Measurement,247,116820-116820.